PDGFRα$^+$ fibroblasts are a major site of cytomegalovirus replication *in vivo* and genome maintenance during latency

Katarzyna M. Sitnik[1], Fran Krstanović[2], Natascha Gödecke[1], Ulfert Rand[1], Tobias Kubsch[1], Henrike Maaß[1], Yeonsu Kim[1], Ilija Brizić[2], Luka Čičin-Šain[1,3,4*]

[1] Department of Viral Immunology, Helmholtz Centre for Infection Research, 38124 Braunschweig, Germany

[2] Center for Proteomics, Faculty of Medicine, University of Rijeka, 51000 Rijeka, Croatia

[3] Centre for individualized Infection Medicine, a joint venture of HZI and MHH, 30625 Hannover, Germany

[4] German Centre for Infection Research (DZIF), Hannover-Braunschweig site, 38124 Braunschweig, Germany

* Corresponding author

Correspondence: Luka Čičin-Šain, Luka.Cicin-Sain@helmholtz.hzi.de

Abstract

Latent cytomegalovirus (CMV) infections affect most of the human population, yet our understanding of the cell types that carry latent CMV *in vivo* remains limited. Here, using the mouse model of latent CMV infection, we comprehensively assessed the prevalence of latent mouse CMV (MCMV) genomes in highly purified populations of fibroblasts, endothelial cells and tissue-resident macrophages across multiple organs upon two distinct infection routes. We describe organ-specific and infection route-specific patterns of viral genome distribution in tissue-resident cells. Strikingly, PDGFRα$^+$ fibroblasts contained the highest MCMV genome load in most organs and conditions analysed. Lytic gene expression was almost completely silenced with only few stochastic transcripts, but the virus *ex vivo* reactivation from PDGFRα$^+$ fibroblasts was consistent and reproducible, arguing that this cell type supports latent infection. Importantly, the same PDGFRα$^+$ fibroblasts supported also the productive

MCMV infection *in vivo*. In sum, these results reveal a role for non-hematopoietic fibroblastic cells as a common site of both lytic MCMV replication and latency *in vivo*.

Introduction

Cytomegalovirus (CMV), a β-herpes virus, is an opportunistic pathogen that chronically infects most of the human population, reaching nearly 100% prevalence in the elderly. CMV is thought to persist in host's cells in a state of latency, which is characterized by the maintenance of viral genomic DNA in the absence of detectable infectious virion production and the ability of viral DNA to reactivate from this state and enter the productive replication cycle under favourable conditions (1). In vivo, latent CMV reactivates in the context of immunosuppression, posing a significant risk of disease and death in individuals suffering from acquired or drug-induced immunosuppression. While latency is well characterized in α and γ herpesviruses, where neuronal cells and B-lymphocytes or endothelial cells have been identified as latency reservoirs, our current understanding of the sites of CMV latency remains limited to cells of the myeloid lineage. On the other hand, tissue-resident and non-hematopoietic cell compartments as potential sites of latent virus presence remain poorly explored.

Our knowledge about CMV latency is based on combined insights from analysis of data from humans naturally infected with human CMV (HCMV) and experimental infection of mice with mouse CMV (MCMV). Virological and immunological properties of both viruses are similar (2). Studies of HCMV latency, which have thus far been exclusively focused on the hematopoietic cell compartment, have characterized monocytes and myeloid $CD34^+$ progenitors as cell types that can be latently infected with HCMV (3-5). Similarly, MCMV genomes were recently detected in monocytes and their progenitors in the bone marrow of latently infected mice (6). In addition, studies in mice have also addressed other potential sources of latent CMV, although in a rather limited manner. Accordingly, studies from the ‘70s to mid ‘90s collectively demonstrated the presence of MCMV genomes and virus reactivation from $F4/80^+$ macrophage-like cells obtained from peritoneum of latently infected mice (7, 8). Experiments of Mercer et al. and Pomeroy et al. performed more than 30 years ago, described enrichment for MCMV genomes and virus reactivation from spleen tissue pieces that sedimented to

the bottom of the tube, while no such activity was registered in the cellular fraction that remained in suspension (9, 10). This indicated that MCMV reactivation may require an intact cell-cell interaction, or that latency is established in splenic fibroblastic and/or endothelial cells. While putative latent infection of fibroblasts has thus far not been confirmed, latent MCMV infection of endothelial cells was observed in the liver (11, 12). In sum, the available data is scattered between different organs and mostly generated before the advent of contemporary cell identification and purification methods. Therefore, the localization of latent MCMV genomes and the relative contribution of various cellular compartments to the pool of infected cells in latency remains unanswered.

Here, we performed a comprehensive analysis of numerous organs and cell subsets in them to determine which organ sites are the most abundant in latency. We report that PDGFRα$^+$ stromal cells have the highest load of viral genomes in latency, a very muted transcriptional profile during latency, and yet the culture of these cells resulted in virus reactivation at approximately 1 week upon explantation, while the PDGFRα$^-$ cell fraction did not. Notably, the PDGFRα$^+$ cells supported virus replication in vitro and in vivo, arguing that the same cell type might be simultaneously a major site of productive virus replication and latency, which would be a new paradigm in herpes virus biology.

Results

Non-hematopoietic cells carry MCMV genomes during latent MCMV infection.

To better characterize the cellular sites of latent CMV infection, we determined MCMV genome load in FACS-sorted fibroblastic-, endothelial-, epithelial- and tissue-resident macrophage populations from the salivary glands (SG), lungs, liver, spleen and visceral adipose tissue (AT) of mice latently infected via intraperitoneal route, as well as from SG and lungs of mice latently infected via intranasal route (Fig. 1a). Populations of tissue-resident macrophages (MF), such as F4/80$^+$CD11c$^+$ SG MF, lung alveolar MF, liver Kupfer cells, spleen red pulp MF and AT MF were identified using organ-specific gating strategies (13-15) (for detailed phenotypes and gating see Fig. 1b-k and Supplementary Fig. 1). Endothelial cells (EC) and fibroblastic cells (FC) were identified respectively as CD45$^-$PDGFRα$^-$CD31$^+$ and CD45$^-$CD31$^-$PDGFRα$^+$ cells in all organs, except that in the liver we focused on a defined

PDGFRα^{+} FC subset, vitamin A^{+} SSC^{hi} liver stellate cells (16) (for detailed phenotypes and gating see Fig. 1b-k and Supplementary Fig. 1). To determine the frequency of MCMV genomes, genomic DNA isolated from sorted cell subsets was used as input in a quantitative PCR assay with primers specific to viral gB gene and to mouse *Pthrp* gene. Absolute quantification was performed using serial dilutions

Figure 1

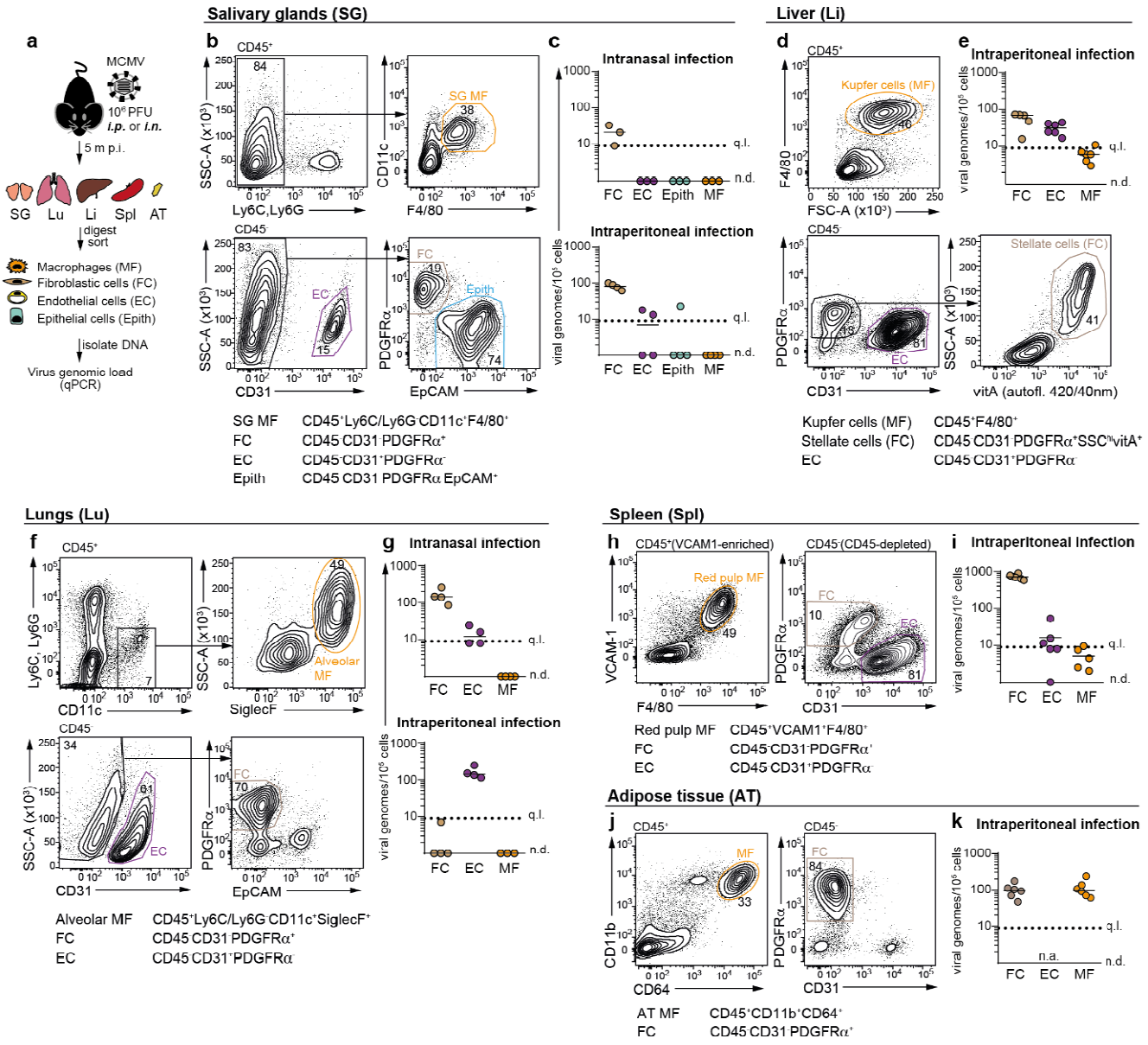

Figure 1. Non-hematopoietic cells carry MCMV genomes during latent MCMV infection. a-k Viral genome load in indicated cell populations across tissues during MCMV latency *in vivo*. SG, submandibular salivary gland; Li, liver; Lu, lungs; Spl, spleen; AT, visceral adipose tissue. **a** Experimental set up. *i.n.,* intranasal. *i.p.,* intraperitoneal. **b, d, f, h, j** Gating strategy for sorting of the indicated cell subsets. Numbers are percentage of cells in the indicated gates. **c, e, g, i, k** MCMV genome load per 10^5 cells. Horizontal line depicts median from 3-6 biological replicates (depicted as symbols) using cells sorted from individual mice (Li, Lu, AT) or from pooled preparations from 2 (SG) or 4 (Spl) mice. q.l., quantification limit; n.d., not detected; n.a., not analysed

of a plasmid carrying both gB and *Pthrp* sequences, according to a previously described method (17), with a quantitation limit of 10 copies of the plasmid standard in a single qPCR reaction (Supplementary Fig. 1g). Overall, MF carried the lowest content of MCMV genomes, with absent or barely detectable levels in SG, lungs, liver and spleen (Fig. 1b-i). A notable exception to this were AT MF, which carried substantially more MCMV genomes than other organs (Fig. 1j-k). In contrast, MCMV genomes were consistently enriched in non-hematopoietic cells (Fig. 1b-k), with AT being the only site, in which viral genomic loads in non-hematopoietic cells and MF were similar (Fig. 1k). Importantly, there were also notable differences in MCMV genomic load between FC and EC. Strikingly, PDGFRα^+ FC were a more prominent source of MCMV genomes than EC in the liver (ca 2-fold), in SG and lungs of mice infected via intranasal route (ca 10-fold) and most substantially, in the spleen (ca 100-fold) (Fig. 1b-k). Only in the lungs of mice infected via intraperitoneal route were MCMV genomes confined to EC and not FC (Fig. 1f-g). Of note, EC from AT were not analysed as they could not be isolated in sufficient numbers. Thus, distinct routes of infection result in differences in MCMV genome distribution between FC and EC in the lungs. Together, these results reveal that MCMV genomes are most abundant in the FC compartment of multiple organs during latency *in vivo*.

The spleen is dispensable for the development of memory CD8$^+$ T cell inflation during MCMV infection.

Given the particularly high MCMV genome load in splenic FC of latently infected mice, we next aimed to more precisely map the distribution of MCMV genomes in this organ. To this end, we fractionated spleen FC into BST-1$^+$ white pulp FC and Ly6C$^+$ red pulp FC (18) and determined their MCMV genome content by qPCR (Fig. 2a-b). Notably, MCMV genome load differed substantially between white-pulp FC and red-pulp FC, with the latter being nearly 10-fold more enriched (Fig. 2c). Given the known importance of non-hematopoietic cells in driving memory CD8$^+$ T cell inflation during MCMV infection (19, 20), we next determined whether splenic FC and the spleen in general played a non-redundant role in this process by monitoring MCMV-specific CD8$^+$ T cell responses in splenectomized mice. To address the role of the spleen respectively in the induction and maintenance of memory inflation, splenectomy was performed either 2 months before the infection (Fig. 2d) or 4 months post

Figure 2

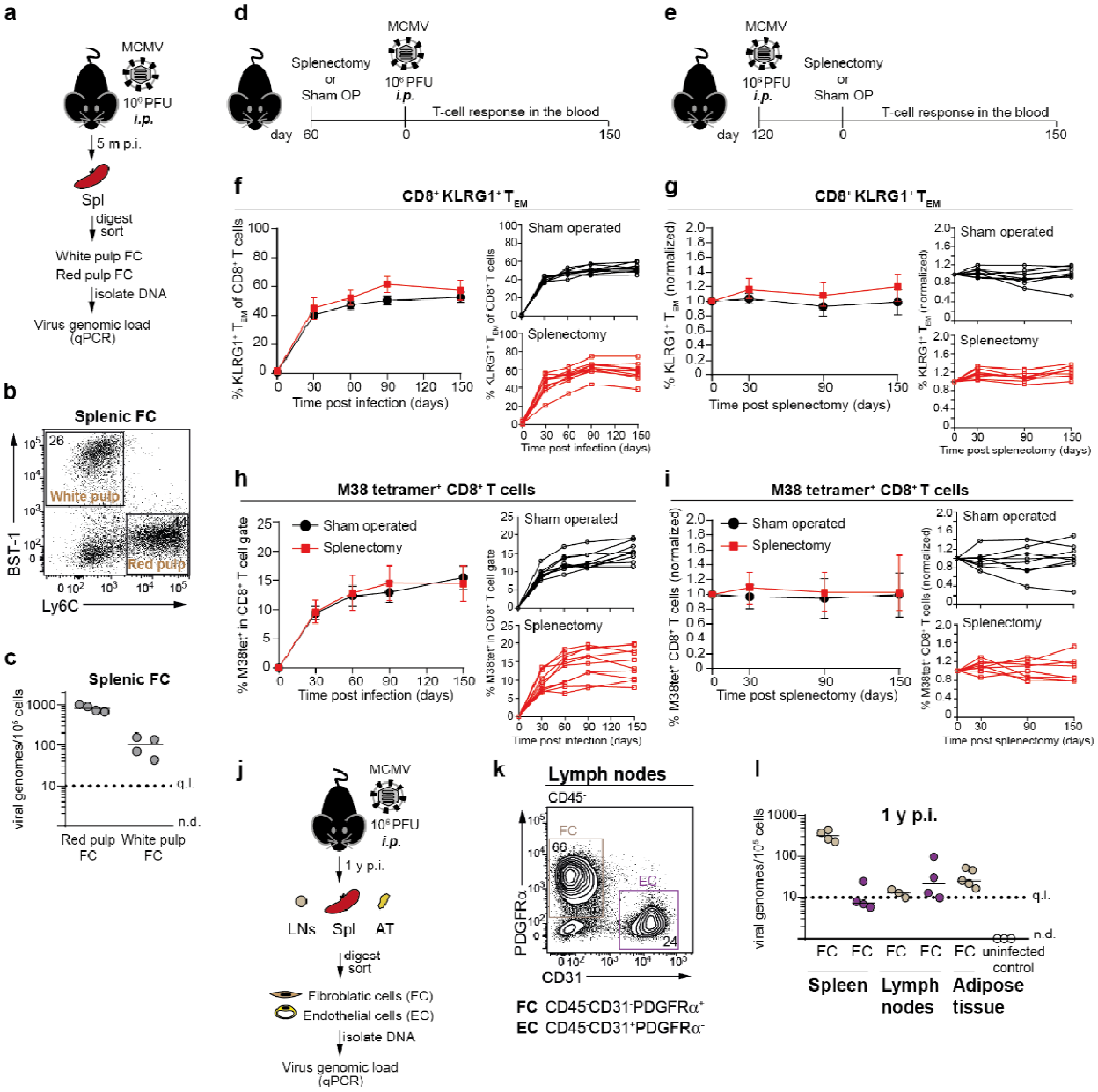

Figure 2. The spleen is dispensable for the development of memory CD8$^+$ T cell inflation during MCMV infection. a-c Viral genome load in splenic white pulp- and red pulp FC during MCMV latency *in vivo*. **a** Experimental set up. **b** Gating strategy for sorting of the indicated cell subsets. Numbers are percentage of cells in the indicated gates. **c** MCMV genome load per 10^5 cells. Data are pooled from 3 independent experiments and are presented as median (horizontal line) of 4 biological replicates (depicted as symbols) using cells sorted from pooled preparations from 2-4 mice per replicate. **d-i** CD8$^+$ T cell response kinetic in the blood following **d, f, h** MCMV-infection of splenectomized or sham operated mice or **e, g, i** splenectomy or sham operation performed on latently infected mice. **d-e** Experimental set up. **f-i** (left) Data are pooled from 8-9 individual mice and are presented as mean (± 95% CI). (right) Data from individual mice. **j-l** Assessment of viral genome load in indicated cell subsets isolated from of latently infected mice 1 year after infection. Lymph nodes (LNs) are pooled inguinal, brachial, axillary, cervical and mesenteric lymph nodes. **j** Experimental set up. **k** Gating strategy for the indicated lymph node subsets. Numbers are percentage of cells in the indicated gates. **l** Data are pooled from 2 (AT) or 3 (LNs, Spl) independent experiments and are presented as median of 3-5 biological replicates (depicted as symbols) using cells sorted from pooled preparations from 2-4 mice per replicate. q.l., quantification limit; n.d., not detected

infection (Fig. 2e), followed by kinetic assessment of the inflationary response in the blood of infected animals for 5 months. Splenectomy had no impact on the percentage of inflationary KLRG1$^+$ CD8$^+$ T effector-memory (T_{EM}) cells (Fig. 2f-g) or the percentage of primed CD8$^+$ cells specific for known inflationary epitopes derived from viral M38 (Fig. 2h-i), m139 (Supplementary Fig. 2c-d) or IE3 (Supplementary Fig. 2e-f). For gating strategies see Supplementary Fig. 2a-b. Thus, the spleen is dispensable for the induction and maintenance of memory CD8$^+$ T cell inflation during MCMV infection. This result suggested that redundancy may exist between the spleen and other lymphoid organs, such as lymph nodes (LNs) in providing viral antigens for T cell restimulation. To address the putative availability of MCMV antigen in the stromal cells of lymph nodes, we quantified the MCMV genome content in non-hematopoietic cell subsets from the LNs, and compared it to the spleen and AT of latently infected mice (Fig. 2j). LN EC (CD45$^-$PDGFRα^-CD31$^+$) and FC (CD45$^-$CD31$^-$PDGFRα^+) were isolated from pooled preparations from inguinal, axillary, brachial, cervical and mesenteric lymph nodes (Fig. 2k). As shown in Fig. 2l, even 1 year after infection, MCMV genomes were present in all non-hematopoietic subsets analysed, with LN EC and FC being similarly enriched as splenic EC and AT FC. These results demonstrate that MCMV genomes are maintained long-term in non-hematopoietic cell populations of both the spleen and the LNs.

MCMV establishes latency in PDGFRα^+ FC

Next, we investigated if PDGFRα^+ FC were a site of latent or persistent MCMV infection. To this end, we first assessed viral mRNA expression in PDGFRα^+ FC isolated from the spleen, liver, SG and AT of mice latently infected via peritoneal route and from the lungs of mice latently infected via intranasal route by RT-qPCR (Table 1). Expression of viral genes from the immediate-early phase of the lytic replication (IE1/IE3), the early (M38) or the late phase (M48/SCP) was used to define if the gene expression was consistent with the lytic viral cycle. The mouse house-keeping gene *Gapdh* served as control, to verify if the overall amount of mRNA was similar in the samples, and evidenced by a very similar ct value for *Gapdh* mRNA in all samples (Table 1). While all samples contained robust and comparable levels of *Gapdh* mRNA, expression of viral mRNAs was detected only sporadically and at very low levels (Table 1). None of the samples expressed all three viral genes (Table 1), consistent

with an intermittent and stochastic viral gene expression during latent MCMV infection (21-24). Specifically, IE1/IE3 was detected in less than 40% of tested samples while M38 and M48/SCP were each detected in less than 10% of tested samples (Table 1). Importantly, our assay specifically detected viral RNA, since no positive signals were obtained when the same samples were processed with omission of reverse-transcriptase (data not shown). Further importantly, PDGFRα^+ FC isolated from the spleen of mice acutely infected with MCMV for 12 hours expressed all three viral genes and the signal was detected 10 PCR cycles earlier than the detectable signals in latently infected mice (Table 1). Thus, the profile of viral gene expression in PDGFRα^+ FC isolated from latently infected mice is not consistent with persistent lytic infection, but rather fits the characteristics of latent infection. To test other functional criteria of latency, we next determined if MCMV can reactivate from PDGFRα^+ FC. This this end, we devised an *ex vivo* reactivation assay, in which PDGFRα^+ FC purified from latently infected mice were seeded in 96-well plates at 10^5 cells per well (ca 70 % confluency after cell attachment). Upon 7 days of *ex vivo* incubation, viral reactivation was assessed in individual wells using three criteria: i) visual inspection of plaque formation, ii) IE1 immunofluorescence as well as iii) detection of infectious virus in culture supernatant by plaque assay on mouse embryonic fibroblasts (MEFs) (Fig. 3a). Importantly, PDGFRα^+ FC isolated from the lungs of mice latently infected via the intranasal route gave rise to reactivated virus in 30-40 % of wells from each biological replicate (Fig. 3b-c). As expected, PDGFRα^+ FC isolated from the lungs of mice latently infected via the intraperitoneal route, did not yield any reactivated virus (Fig. 3b), as they were shown to be devoid of MCMV genomes (see Fig. 1g). To confirm these results in FC from another tissue, but also to study the timing of virus reactivation, reactivation was also monitored in PDGFRα^+ FC isolated from AT of mice latently infected with recombinant MCMV expressing IE promoter-driven GFP, MCMV$^{IE1/3\text{-}GFP}$ via the intraperitoneal route. Cells were monitored for the emergence of GFP$^+$ plaques by life cell imaging (Fig. 3d). By 7 days of *in vitro* incubation, MCMV reactivated in 9 out of 10 biological replicates with the frequency of 1-2 wells out of 12 wells per replicate (Fig. 3e-f). Most reactivations were initiated 1.5-2 days or 4-5 days after seeding as indicated by the emergence of first GFP$^+$ cells (Fig. 3g and

Supplementary Videos 1-2), arguing against virus persistence and for a state where lytic gene expression had to be re-initiated. Although the purity of sorted PDGFRα$^+$ FC was routinely >95%, we nonetheless addressed the unlikely possibility that the virus only propagated on FC following reactivation from contaminating PDGFRα$^-$ FC, by monitoring virus reactivation in the sorted PDGFRα$^-$ fraction. This possibility was ruled out, because no virus reactivation was detected when PDGFRα$^-$ cells purified from AT of latently infected mice were cultured on a monolayer of PDGFRα$^+$ FC from uninfected mice (Supplementary Fig. 2g-h). Together, these results indicate that MCMV establishes latent infection in PDGFRα$^+$ FC *in vivo*.

Table 1

Viral gene transcription in PDGFRα$^+$ FC from latently-infected mice (RT-qPCR)

		MCMV genome copies per 10e5 cells	Gapdh ct	IE1/3 ct	M38 ct	M48/SCP ct
uninfected	Spl FC	n.a.	21.18 (2/2)	n.d. (0/2)	n.d. (0/2)	n.d. (0/2)
12 h p.i.	Spl FC	n.a.	22.45 (2/2)	22.91 (2/2)	22.00 (2/2)	25.18 (2/2)
latently infected mice (5 months p.i.)	Spl FC	963	20.81 (2/2)	n.d. (0/3)	n.d. (0/3)	n.d. (0/3)
		767	21.23 (2/2)	n.d. (0/3)	n.d. (0/3)	n.d. (0/3)
		673	21.64 (2/2)	n.d. (0/3)	n.d. (0/3)	n.d. (0/3)
	Lu FC	255	21.70 (2/2)	33.89 (3/3)	n.d. (0/3)	n.d. (0/3)
		140	20.17 (2/2)	32.59 (3/3)	37.19 (2/3)	n.d. (1/3)
		148	19.94 (2/2)	32.28 (3/3)	n.d. (0/3)	n.d. (0/3)
	SG FC	100	20.82 (2/2)	n.d. (0/3)	n.d. (0/3)	n.d. (0/3)
		89	21.16 (2/2)	33.88 (3/3)	n.d. (0/3)	n.d. (0/3)
		74	20.63 (2/2)	n.d. (1/3)	n.d. (0/3)	35.76 (2/3)
	Li FC	73	20.52 (2/2)	n.d. (0/3)	n.d. (0/3)	n.d. (0/3)
		48	21.75 (2/2)	n.d. (0/3)	n.d. (0/3)	n.d. (0/3)
		69	20.49 (2/2)	n.d. (0/3)	n.d. (0/3)	n.d. (0/3)
	AT FC	70	20.46 (2/2)	n.d. (0/2)		
		92	20.95 (2/2)	n.d. (0/2)		
		174	21.06 (2/2)	35.4 (2/2)		
		47	21.17 (2/2)	36.6 (2/2)		

Table 1. Expression of MCMV genes in PDGFRα$^+$ FC from latently infected mice. RT-qPCR analysis of the expression of MCMV genes in the indicated subsets. SG, submandibular salivary gland; Li, liver; Lu, lungs; Spl, spleen; AT, visceral adipose tissue. Each row represents a different biological replicate established from cells sorted from individual mice (AT, Li, Lu) or from pooled preparations from 2 (SG) or 4 (Spl) mice. Shown are mean ct values for indicated transcripts. Samples with detectable MCMV transcripts are marked in red. Shown in brackets is the proportion of positive detections per total number of technical replicates analysed.

Figure 3

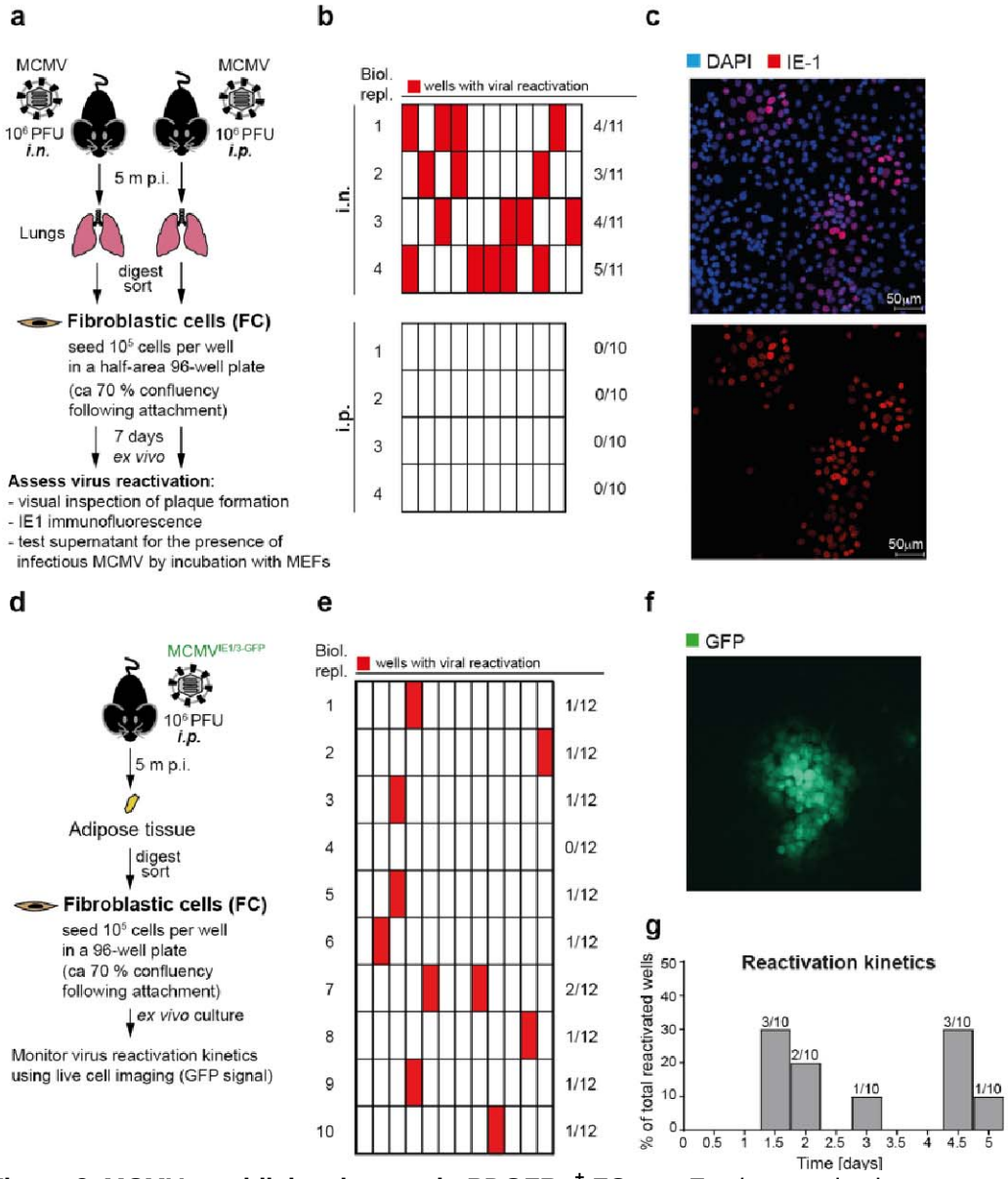

Figure 3. MCMV establishes latency in PDGFRα$^+$ FC. a-c *Ex vivo* reactivation assay using PDGFRα$^+$ FC purified from the lungs of latently infected mice. **a** Experimental set up. **b** Each quadrant represents a single well, in which 10^5 PDGFRα$^+$ FC were seeded. Each row of wells is a different biological replicate set up using PDGFRα$^+$ FC sorted from 1-2 lungs per replicate. Wells positive for virus reactivation are marked in red. Shown to the right is the proportion of positive wells of all wells per biological replicate. **c** Representative immunofluorescence image showing plaques expressing viral IE1 protein that arose in *ex vivo* reactivation assay. **d-g** Live monitoring of viral reactivation in *ex vivo* cultured PDGFRα$^+$ FC purified from visceral adipose tissue of mice latently infected with MCMV$^{ie1/3\text{-}GFP}$. **d** Experimental set up. **e** Each quadrant represents a single well, in which 10^5 PDGFRα$^+$ FC were seeded. Each row of wells is a different biological replicate set up using PDGFRα$^+$ FC sorted from 2 mice per replicate. Wells positive for virus reactivation are marked in red. Shown to the right is the proportion of positive wells of all wells per biological replicate. **f** Representative fluorescence microscopy image of a GFP$^+$ plaque that arose in *ex vivo* reactivation assay. **g** Kinetic of reactivations since the start of *ex vivo* culture. Bars represent the fraction of all positive wells with GFP signal emerging at the indicated time point.

PDGFRα$^+$ FC support productive MCMV infection *in vitro* and *in vivo*

The apparent latency of MCMV in PDGFRα$^+$ FC was puzzling. Fibroblasts and stromal cells are well-known to support lytic MCMV replication and are commonly used to grow virus stocks. Intriguingly, our PDGFRα$^+$ FC appeared to not only be able to carry latent MCMV genomes but also become lytically infected since they supported replication of MCMV and plaque formation upon reactivation (see Fig. 3c, f). To directly assess the permissiveness of PDGFRα$^+$ FC for lytic MCMV infection, we purified PDGFRα$^+$ FC from the lungs of naive mice and infected them *ex vivo* with recombinant MCMV$^{tFP\text{-}GRB}$, which expresses IE promoter-driven green fluorescent protein (GFP) and late gene promoter-driven red fluorescent protein (mCherry) (Fig. 4a). Analysis of viral replication kinetics demonstrated that PDGFRα$^+$ FC can indeed support productive replication of MCMV (Fig. 4b-c). Next, to address if PDGFRα$^+$ FC contributed to MCMV propagation *in vivo*, we infected *Pdgfra*-CreER^{T2} knock-in mice with a Cre-inducible reporter virus, MCMV$^{floxSTOP\text{-}GFP}$ (25). This genetic system was used previously with Tie2-Cre or Alb-Cre mice to define virus replication in endothelial cells or in hepatocytes (26), and is based on the selective deletion of the stop cassette in the viral genome in cells that express the Cre recombinase. Therefore, the viruses that replicate in PDGFRα$^+$ FC and all their progeny were genetically recombined and formed GFP$^+$ plaques when titrated on monolayers of permissive cells. As depicted in Fig. 4d, *Pdgfra*-CreER^{T2} mice were infected with MCMV$^{floxSTOP\text{-}GFP}$ via the peritoneal route on day 0, fed tamoxifen from -1 to 3 days post infection to activate the Cre recombinase, and sacrificed on day 4 post infection. Organ lysates from the adipose tissue, lungs, spleen and liver were used to determine the ratio of GFP$^+$/GFP$^-$ plaques. GFP$^+$ virus was detected as ~10% of plaques in the liver, ~20 % in the adipose tissue and ~50 % in the spleen and lungs, although in the latter organ the percentage of GFP$^+$ plagues could only be reliably measured in 5 out of 10 samples due to generally low infectious virus titer in this organ (Fig. 4e-f). The emergence of GFP$^+$ virus was entirely dependent on Cre recombinase since no GFP$^+$ plaques were found in organs of infected Cre-negative littermate controls (data not shown). These results demonstrated that PDGFRα$^+$ FC play a role in MCMV *in vivo* replication and suggested that they contribute to virus *in vivo* pathogenesis.

Figure 4

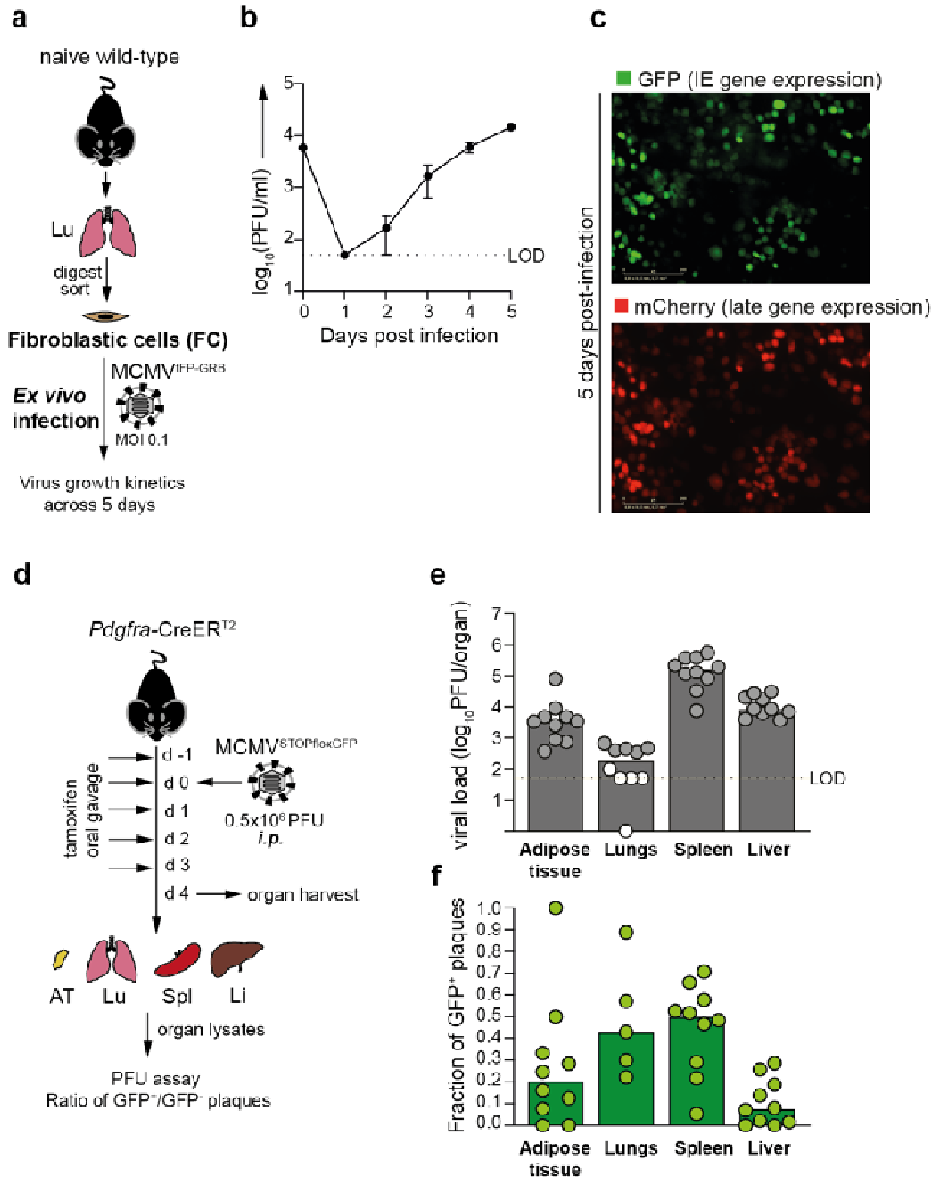

a-c Viral replication kinetics following *ex vivo* infection of primary lung-derived PDGFRα$^+$ FC with MCMV$^{tFP\text{-}GRB}$, which expresses IE promoter driven-green fluorescent protein (GFP) and late gene promoter-driven red fluorescent protein (mCherry). **a** Experimental set up. **b** Data are presented as arithmetic mean ± SD of 3 technical replicates and are from one representative experiment of 2 using cells sorted from pooled lung preparations from 3 mice per experiment. **c** Representative fluorescence microscopy images of GFP and mCherry expression 5 days following *ex vivo* infection. **d-f** Contribution of PDGFRα$^+$ FC to MCMV propagation *in vivo* determined after intraperitoneal infection of *Pdgfra*-CreER^{T2} mice with a Cre-inducible reporter virus, MCMV$^{floxSTOP\text{-}GFP}$. **d** Experimental set up. **e** Median virus titer in indicated organs. Circles represent samples from individual mice. Grey-filled circles are samples for which percentage of GFP$^+$ plaques could be determined. White-filled circles are samples for which percentage of GFP$^+$ plaques could not be determined. **f** Median proportion of GFP$^+$ plaques in indicated organs. Circles represent samples from individual mice.

In sum, PDGFRα^+ FC supported both the productive and the latent MCMV infection *in vivo,* arguing that the same cell type is used by a herpesvirus for lytic and latent infection, depending on the circumstances.

Discussion

This work is to our knowledge the first effort at a comprehensive analysis of cellular sites that may harbour latent CMV. While it is understood that our work did not address each and every organ and cellular site in the body, we targeted our efforts towards the organs that were frequently considered in the study of virus latency. We identified viral genomes in macrophages and endothelial cells, in line with previous reports (6, 7, 11, 24), but we also identified the stromal cells as a major contributor to the pool of latent genomes. It is notable that viral genomes in fibroblastic cells were transcriptionally muted and expressed only few transcripts, predominantly immediate-early ones, in line with previous reports (22, 27, 28). Furthermore, upon explantation, the GFP signal was not immediately detectable (Fig. 3), although the GFP gene in our recombinant virus was driven by the endogenous promoter of the immediate-early gene (29). Therefore, our data argue against a persistent virus replication, and fit within the formal definition of virus latency.

In a recent report by Munks *et al*. it was shown that endothelial cells contribute to the induction of inflationary CD8$^+$ T cells recognizing viral epitopes during latency, but are not the sole source of virus antigen (30). Our work fits with this report, as we observed viral genomes in both endothelial and fibroblastic cells in lymph nodes and in the spleen. However, our data do not provide evidence if the latent transcription in PDGFRα^+ FC provides antigens for the induction of memory inflation, and this aspect needs to be explored in a detailed subsequent study. In light of the high abundance of viral genomes in the splenic red pulp stroma, we explored the contribution of these cells and this organ to memory inflation, and observed that they are not necessary. This is consistent with the report by Munks *et al*. who showed that latent antigen in endothelial cells may be sufficient, but is not necessary for memory inflation, but also with data, where thymectomy or sialoadenectomy also failed to alter the dynamics of memory inflation (31). Taken together, the reports would be consistent with a model,

where multiple organs contribute to the pool of antigens expressed in latency, but no single organ or cell type is responsible for the antigen induction of inflationary cells. This however, would need to be definitely confirmed in highly comprehensive future studies.

Another limitation of our study is that we could not identify a definite transcriptional program in PDGFRα^+ FC harbouring viral genomes in latency. Latency associated transcripts were described in herpes simplex infection and latency associated proteins are well known in gamma herpesviruses (32-35). Furthermore, it has been shown that myeloid cells that harbour HCMV genomes have a programmed and transcriptional program that acts as an alternative to the lytic gene expression program (36). Our study was not conceived to define viral latency at this level of detail, which would require enrichment of latently infected cells followed by transcriptome analyses at bulk and single-cell levels, but this work can now be performed, as we have identified the cell type to focus on.

Similarly, our data raises the question if HCMV genomes may also be identified in human stromal cells. While the blood compartment has been exceptionally well studied due to the mere availability and ease of acquisition of samples, no firm results are available for other compartments of the human body. A notable exception is a short study by Reeves *et al*. (37), who addressed HCMV latency in endothelial cells of large veins, but failed to identify any viral nucleic acids. However, the relative lack of evidence cannot be construed as evidence of lack. Therefore, the contribution of non-hematopoietic cells to the latent reservoir in humans remains an open question. Our results point towards stromal cells as cell types that may support virus maintenance in latency and argue that this is not mutually exclusive with the site supporting productive virus infection.

Methods

Mice

Experiments were performed with 8-10 weeks-old mice on C57BL/6 background. Female mice were used in all experiments except in Fig. 4 wherein 6-8 weeks old mice of both sexes were used. C57BL/6JrJ mice were purchased from Janvier Labs. *Pdgfra*^{CreER} mice (38) were purchased from the Jackson Laboratory (JAX stock #032770). Mice were bred and maintained at central animal facilities

at HZI Braunschweig, Germany or at Faculty of Medicine, University of Rijeka, Croatia under specific pathogen free conditions according to Federation of European Laboratory Animal Science Associations (FELASA) guidelines. Animal procedures were approved as due by The Lower Saxony State Office of Consumer Protection and Food Safety, or by The Ethics Committee at the Faculty of Medicine, Rijeka and Ethics Committee of the Veterinary Department of the Ministry of Agriculture, Croatia.

Viral infection of mice

Cohorts of latently infected animals were generated by infecting mice with 10^6 PFU of bacterial artificial chromosome (BAC)–derived $MCMV^{wt}$ (clone pSM3fr-MCK-2fl 3.3 (39)) or recombinant MCMV-GFP-P2A-ie1/3, $MCMV^{IE1/3\text{-}GFP}$ (18). Virus diluted in 200 µl PBS was i.p. injected. Virus solution (20 µl in PBS) was administered into both nostrils of mice under anaesthesia as described previously (40). Viral stocks were generated in tissue culture by transfecting recombinant BACs into NIH3T3 cells (ATCC CRL-1658) using FuGene HD (Promega, USA) and passaging of reconstituted viral particles five times before generating a stock from infected M2-10B4 mouse fibroblastic cells (ATCC CRL-1972). For analysis of the *in vivo* sites of MCMV replication, 6-8 weeks old *Pdgfra*-$CreER^{T2}$ mice and littermate Cre-negative control mice were i.p. infected on day 0 with 0.5 $x10^6$ PFU of $MCMV^{floxSTOP\text{-}GFP}$ (25). Mice received daily from day -1 to day 3 tamoxifen (Sigma, Cat# T5648-5G) diluted in corn oil (Sigma, Cat# C8267-500ML) by oral gavage. On day 4 after infection animals were sacrificed, and viral titer in organs determined by plaque assay as described previously (41). Number of GFP^+ plaques was determined using a fluorescence microscope (Olympus). Only plaques visible in bright field were considered for the calculation.

Splenectomy

Splenectomy was performed on anesthetized mice 2 months before or 4 months after infection with 10^6 PFU of BAC-derived $MCMV^{wt}$ (clone pSM3fr-MCK-2fl 3.3 (39)) i.p. A dorsal incision was made lateral to the spine and the abdominal cavity was entered. The splenic blood vessels were ligated, and the spleen was removed by transecting the vessels just distal to the ligature. Peritoneum and skin were closed by surgical stitches.

Cell Isolation

Peripheral blood was harvested, and lymphocytes were isolated as described previously (40). Spleen, lymph nodes and salivary glands were digested with collagenase P (0.4 mg/ml), dispase II (2 mg/ml) and DNase I (50 µg/ml) in RPMI-1640 supplemented with 1 mM sodium pyruvate, 100 U/ml penicillin, 100 U/ml streptomycin, 10 mM HEPES and 5 % fetal bovine serum (FBS), according to a previously established protocol (18). Briefly, enzymatic treatment was performed for 30 min at 37 °C and then repeated for additional 20 min, followed by incubation with 5 mM EDTA for 5 min. For sorting of splenic stromal cells or red pulp macrophages, the cell suspension was respectively subjected to immunomagnetic depletion of $CD45^+$ cells or to positive selection of $VCAM\text{-}1^+$ cells using MACS (Miltenyi Biotech). Lungs were collected after perfusion of mice via the right ventricle with 10 ml PBS. Dissected organs were injected with 2.5 ml digestion solution containing collagenase P (0.4 mg/ml), dispase II (2 mg/ml) and DNase I (50 µg/ml) and cut into pieces with scissors. Subsequently, tissue pieces were transferred into the gentleMACS C Tube containing 2.5 ml of fresh digestion medium and digested in the gentleMACS Dissociator (Miltenyi Biotech) using the manufacturer's program "37C_m_LDK_1". Stromal-vascular fractions from peri-gonadal VAT were prepared as described (42) with modifications. Briefly, adipose tissue was digested with collagenase P (0.4 mg/ml), dispase II (2 mg/ml) and DNase I (50 µg/ml) in high-glucose GlutaMAX-supplemented DMEM with 10 mM HEPES and 4% fatty acid-free BSA (Sigma-Aldrich) for 55 min at 37°C. The suspension was passed through a 100 µm nylon mesh filter (BD Biosciences), and the floating adipocyte fraction was removed by centrifugation at 400 × g for 6 min. Liver digestion was performed using the retrograde perfusion technique via the inferior vena cava described by Mederacke *et al*. (43) with modifications. Briefly, organs were *in situ* perfused with 10 ml of pre-warmed Liver Perfusion Medium (Gibco) followed by the injection of 20 ml of pre-warmed digestion medium (1 mg/ml collagenase P, 1 mg/ml dispase II, 50 µg/ml DNase I in Gibco Hank's Balanced Salt Solution (HBSS) with 10 mM HEPES and 1.5 mM calcium chloride) over 5-7 min. Afterwards, organs were dissected, minced with scissors and *in vitro* digested for 45 min at 37°C. The resulting cell suspension was passed through a 100 µm nylon mesh filter (BD Biosciences). Subsequently, non-parenchymal cells were enriched by two rounds of

centrifugation at 50 × g for 5 min whereupon only the supernatant was collected. Prior to staining with antibodies, cell suspensions were subjected to red blood cell lysis using ACK lysing buffer prepared in-house (0.15 M ammonium chloride, 0.01 M potassium bicarbonate, 0.0001 M disodium EDTA dissolved in water).

Flow Cytometry and Cell Sorting

Flow cytometry was performed with antibodies (listed in Supplementary Table 1) according to standard procedures (44). Dead cells (identified using 7-AAD Viability Staining Solution or Zombie NIR Fixable Viability Kit; both from BioLegend) and cell aggregates (identified on FSC-A versus FSC-H scatter plots) were excluded from all analyses. Data acquisition was performed on an Aria-II SORP, ARIA-Fusion or LSR-Fortessa (BD Biosciences) and analysed using FlowJo software (BD Biosciences). Sorting was performed on an Aria-II SORP or ARIA-Fusion (BD Biosciences).

For quantification of MCMV-specific T cell responses cells were incubated with APC-conjugated M38, APC-conjugated IE3 or PE-conjugated m139 tetramers (kindly provided by Ramon Arens, Department of Immunology, Leiden University Medical Center, Leiden, Netherlands) for 30 min at room temperature, and subsequently stained with antibodies for 30 min at 4°C.

Quantification of MCMV and mouse genome copies

Total DNA was extracted using AllPrep DNA/RNA Micro Kit (QIAGEN). Each sample of eluted DNA was precipitated with ethanol, washed, and resuspended in 40 µl dH_2O. Quantification of MCMV and mouse genome copies was performed as described previously (17). Viral gB and mouse Pthrp sequences were assayed in technical duplicates using 9 µl of sample DNA per reaction. Serial dilutions of 10^1-10^6 copies per reaction of the pDrive_gB_PTHrP_Tdy plasmid (17) were used to generate standard curves for both qPCR reactions. Dilutions of 10^1-10^4 plasmid copies contained 1 ng carrier RNA (QIAGEN). Quantitative PCR was performed using Fast Plus EvaGreen qPCR master mix (Biotium) in a LightCycler 480 Instrument II (Roche). Cycling conditions were as follows: enzyme activation, 2 min 95°C, followed by 50 cycles of denaturation for 10 sec at 95°C, annealing for 20 sec at 56°C and extension for 30 sec at 72°C. Specificity of amplified sequences was validated for all samples in each run by the inspection of the respective melting curve profiles.

Primer sequences:

Pthrp forward 5'-ggtatctgccctcatcgtctg-3' and reverse 5'-cgtttcttcctccaccatctg-3'

gB forward 5'-gcagtctagtcgctttctgc-3' and reverse 5'-aaggcgtggactagcgataa-3'

RT-qPCR

Total RNA was extracted using AllPrep DNA/RNA Micro Kit (QIAGEN), reverse transcribed with SuperScript IV and a 1:1 mixture of oligo-dT and random oligonucleotide hexamers (all from Thermo Fisher). Quantitative PCR was performed using Forget-Me-Not EvaGreen qPCR Master Mix (Biotium) in a LightCycler 480 Instrument II (Roche). The efficiency of each primer pair was validated for the use of the $2^{-\Delta CT}$ method using serially diluted cDNA from acutely infected splenic FC. The absence of contaminating viral DNA in all RNA preparations was verified by running in parallel RT-qPCR reactions prepared from an equal amount of RNA but with the omission of reverse transcriptase.

Primer sequences:

Gapdh forward 5'-tgtgtccgtcgtggatctga-3' and reverse 5'-cctgcttcaccaccttcttgat-3'

ie1/3 forward 5'-gggcatgaagtgtgggtaca-3' and reverse 5'-cgcatcgaaagacaacgcaa-3'

M38 forward 5'-cccatgtccacgttttggtg-3' and reverse 5'-tctcaagtgcaatcgcctca-3'

M48/SCP forward 5'-aggacgtgttgaacttcttctcc-3'and reverse 5'-tcgatgtccgtctccttcac-3'

***Ex vivo* Reactivation Assays**

PDGFRα^+ FC that had been FACS-sorted from the lungs of latently infected mice were seeded into fibronectin-coated 96 Half Area Well Flat Bottom Microplates (Corning, Cat# 3696) at a density of 100,000 cells per well in 100 µl of culture medium (high-glucose DMEM (Gibco, Cat # 11995065) supplemented with 1 % (vol/vol) GlutaMAX, 10 mM HEPES, 50 µM 2-mercaptoethanol, 200 U/ml penicillin, 200 U/ml streptomycin, 50 µg/ml gentamicin and 5 % FCS). Adipose tissue-derived PDGFRα^+ FC were seeded into gelatin- or fibronectin-coated 96 Well Flat Bottom Microplates (Greiner Bio-One, Cat# 655160) at a density of 100,000 cells per well in 200 µl of culture medium. Cells were incubated and imaged with Sartorius IncuCyte S3 automated fluorescence microscope in a humidified incubator under 5 % CO_2 and at 37°C for 7 days without replacing the medium. Infectious virus was

detected by incubation of culture supernatants with primary mouse embryonic fibroblasts (MEFs) prepared in-house from C57BL/6JrJ mice. Briefly, the entire volume of culture supernatant from each well (~100 µl) was transferred into another well of a 96-well plate carrying a monolayer of MEFs. To ensure detection of even minimal amounts of virus (28), infection was enhanced by centrifugating the plates at 2000 rpm for 30 min prior to incubation at 37°C for another 30 min. Thereupon, the inoculum was removed and the cells overlaid with 0.75 % (wt/vol) carboxymethylcellulose (Sigma) in Eagle's minimal essential medium (Gibco) supplemented with 5 % FCS (Sigma), 2 mM L-glutamine, 1 % (vol/vol) MEM Non-Essential Amino Acids Solution (Gibco) and 1.5 % (wt/vol) sodium bicarbonate. The cells were incubated at 37□°C for 4 days, and the plaques were examined under an inverted microscope.

IE1 Immunofluorescence Staining

Cells were fixed in 4 % (wt/vol) paraformaldehyde (PFA) for 10 min at room temperature (RT). thereupon, the cells were permeabilized in 0.1% Triton-X in PBS for 15 min at RT and treated with blocking solution (PBS containing 2% BSA and 0.05% Tween-20) for an hour at RT to block nonspecific antibody binding. Afterwards, the cells were incubated with anti-IE1 antibody (IE 1.01, CapRi, Rijeka, Croatia) diluted in blocking solution overnight at 4˚C. Primary antibody binding was visualized with anti-mouse IgG (H+L) $F(ab')_2$ Fragment conjugated to Alexa Fluor 647 (Cell Signaling Technology, MA, USA) in blocking solution for an hour at RT. Images were acquired with ZEISS LSM 980 laser-scanning confocal microscope and analysed using ZEN software (both from Carl Zeiss MicroImaging).

***Ex vivo* infection of cells**

$MCMV^{tFP\text{-}GRB}$ expressing three different fluorescent proteins under the control of endogenous viral promoters is based on the Mck2-repaired BAC-encoded Smith strain (39, 45) and was generated by *en passant* mutagenesis (46) using expression cassettes described earlier (47). In short, fluorescent reporter genes were inserted into the start codon of IE1/3 (eGFP), E2 (mTagBFP-NLS), and SCP (mCherry) with a 2A-peptide encoding sequence. Therefore, fusion transcripts of reporter and viral gene are generated upon viral promoter activation and translation products (unaltered viral factor and

fluorescent protein) become separated by ribosomal frameshifting. PDGFRα^+ FC from lungs of naive mice were seeded into fibronectin-coated 96 Half Area Well Flat Bottom Microplates (Corning, Cat# 3696) in culture medium (high-glucose DMEM (Gibco, Cat # 11995065) supplemented with 1 % (vol/vol) GlutaMAX, 10 mM HEPES, 50 µM 2-mercaptoethanol, 200 U/ml penicillin, 200 U/ml streptomycin, 50 µg/ml gentamicin and 5 % FCS) and incubated at 37°C for 48 hours until the cells reached 80 % confluency. Cells were then infected with MCMV$^{tFP\text{-}GRB}$ at an MOI of 0.1 for an hour at 37°C. Afterwards, the medium was changed to cultivation medium without virus. Supernatant was collected from a different set of wells every 24 hours until 5 days post infection and stored at -80°C until further processing. GFP and RFP fluorescence was imaged with Sartorius IncuCyte S3 automated fluorescence microscope. The infectious titer was determined by serially diluting the supernatants and then infecting MEF cell monolayers in 48-well plates for an hour at 37□°C. Thereupon, the inoculum was removed, and the cells were overlaid with 0.75 % methylcellulose. The cells were incubated at 37□°C for 4 days, and the plaques were counted under an inverted microscope.

Acknowledgements

This study was funded by the Deutsche Forschungsgemeinschaft (DFG, German Research Foundation) – Projektnummer 158989968 - SFB 900 and the RESIST Excellence cluster (EXC 2155, project B6), the German Centre for Infection Research (DZIF) of the German Federal Ministry of Science and Education (BMBF) through TTU 07.834 (to L.C-S.), the European Union's Horizon 2020 research and innovation program under Grant Agreement 793858 (to K.M.S.). Ilija Brizić is supported by "Research Cooperability" program of the Croatian Science Foundation funded by the European Union from the European Social Fund under the "Operational Programme Efficient Human Resources 2014–2020" (PZS-2019-02-7879). We thank Inge Hollatz-Rangosch and Ayse Barut for technical assistance. We acknowledge Lothar Gröbe and Maria Höxter from HZI core flow cytometry facility, Marina Pils, Katrin Schlarman and Petra Beyer from the animal house, as well as Robert Geffers from HZI genomics platform.

Author contributions

Concept and study design, K.M.S. and L.C-S.; Investigation, K.M.S., F.K., N.G., H.M., Y.K.; Methodology, K.M.S. and L.C-S., Materials: U.R. and T.K.; Resources, L.C-S. and I.B.; Funding acquisition, L.C-S., K.M.S., I.B.; Writing of the manuscript, K.M.S. and L.C-S.; Supervision, L.C-S.

Competing interests

L.C-S. has submitted a patent for the use of CMV as a vaccine vector. The authors declare no further competing interests.

References

1. Reddehase MJ, Lemmermann N. Cytomegaloviruses: From Molecular Pathogenesis to Intervention: Caister Academic Press; 2013.
2. Podlech J, Holtappels R, Grzimek NKA, Reddehase MJ. Animal models: Murine cytomegalovirus. Methods in Microbiology. Volume 32: Academic Press; 2002. p. 493-IN11.
3. Söderberg-Nauclér C, Fish KN, Nelson JA. Reactivation of Latent Human Cytomegalovirus by Allogeneic Stimulation of Blood Cells from Healthy Donors. Cell. 1997;91(1):119-26.
4. Hahn G, Jores R, Mocarski ES. Cytomegalovirus remains latent in a common precursor of dendritic and myeloid cells. Proc Natl Acad Sci U S A. 1998;95(7):3937-42.
5. Taylor-Wiedeman J, Sissons JG, Borysiewicz LK, Sinclair JH. Monocytes are a major site of persistence of human cytomegalovirus in peripheral blood mononuclear cells. The Journal of general virology. 1991;72 (Pt 9):2059-64.
6. Liu XF, Swaminathan S, Yan S, Engelmann F, Abbott DA, VanOsdol LA, et al. A novel murine model of differentiation-mediated cytomegalovirus reactivation from latently infected bone marrow haematopoietic cells. J Gen Virol. 2019;100(12):1680-94.
7. Brautigam AR, Dutko FJ, Olding LB, Oldstone MB. Pathogenesis of murine cytomegalovirus infection: the macrophage as a permissive cell for cytomegalovirus infection, replication and latency. J Gen Virol. 1979;44(2):349-59.
8. Pollock JL, Presti RM, Paetzold S, Virgin HWt. Latent murine cytomegalovirus infection in macrophages. Virology. 1997;227(1):168-79.
9. Mercer JA, Wiley CA, Spector DH. Pathogenesis of murine cytomegalovirus infection: identification of infected cells in the spleen during acute and latent infections. J Virol. 1988;62(3):987-97.
10. Pomeroy C, Hilleren PJ, Jordan MC. Latent murine cytomegalovirus DNA in splenic stromal cells of mice. J Virol. 1991;65(6):3330-4.
11. Seckert CK, Renzaho A, Tervo HM, Krause C, Deegen P, Kühnapfel B, et al. Liver sinusoidal endothelial cells are a site of murine cytomegalovirus latency and reactivation. J Virol. 2009;83(17):8869-84.
12. Dağ F, Dölken L, Holzki J, Drabig A, Weingärtner A, Schwerk J, et al. Reversible Silencing of Cytomegalovirus Genomes by Type I Interferon Governs Virus Latency. PLoS pathogens. 2014;10(2):e1003962.
13. Thom JT, Walton SM, Torti N, Oxenius A. Salivary gland resident APCs are Flt3L- and CCR2-independent macrophage-like cells incapable of cross-presentation. Eur J Immunol. 2014;44(3):706-14.

14. Scott CL, T'Jonck W, Martens L, Todorov H, Sichien D, Soen B, et al. The Transcription Factor ZEB2 Is Required to Maintain the Tissue-Specific Identities of Macrophages. Immunity. 2018;49(2):312-25.e5.
15. Bellomo A, Mondor I, Spinelli L, Lagueyrie M, Stewart BJ, Brouilly N, et al. Reticular Fibroblasts Expressing the Transcription Factor WT1 Define a Stromal Niche that Maintains and Replenishes Splenic Red Pulp Macrophages. Immunity. 2020;53(1):127-42.e7.
16. Mederacke I, Dapito DH, Affò S, Uchinami H, Schwabe RF. High-yield and high-purity isolation of hepatic stellate cells from normal and fibrotic mouse livers. Nature protocols. 2015;10(2):305-15.
17. Simon CO, Seckert CK, Dreis D, Reddehase MJ, Grzimek NK. Role for tumor necrosis factor alpha in murine cytomegalovirus transcriptional reactivation in latently infected lungs. J Virol. 2005;79(1):326-40.
18. Pezoldt J, Wiechers C, Erhard F, Rand U, Bulat T, Beckstette M, et al. Single-cell transcriptional profiling of splenic fibroblasts reveals subset-specific innate immune signatures in homeostasis and during viral infection. Commun Biol. 2021;4(1):1355.
19. Torti N, Walton SM, Brocker T, Rülicke T, Oxenius A. Non-hematopoietic cells in lymph nodes drive memory CD8 T cell inflation during murine cytomegalovirus infection. PLoS Pathog. 2011;7(10):e1002313.
20. Seckert CK, Schader SI, Ebert S, Thomas D, Freitag K, Renzaho A, et al. Antigen-presenting cells of haematopoietic origin prime cytomegalovirus-specific CD8 T-cells but are not sufficient for driving memory inflation during viral latency. Journal of General Virology. 2011;92(9):1994-2005.
21. Grzimek NK, Dreis D, Schmalz S, Reddehase MJ. Random, asynchronous, and asymmetric transcriptional activity of enhancer-flanking major immediate-early genes ie1/3 and ie2 during murine cytomegalovirus latency in the lungs. J Virol. 2001;75(6):2692-705.
22. Simon CO, Holtappels R, Tervo HM, Bohm V, Daubner T, Oehrlein-Karpi SA, et al. CD8 T cells control cytomegalovirus latency by epitope-specific sensing of transcriptional reactivation. J Virol. 2006;80(21):10436-56.
23. Reddehase MJ, Simon CO, Seckert CK, Lemmermann N, Grzimek NK. Murine model of cytomegalovirus latency and reactivation. Curr Top Microbiol Immunol. 2008;325:315-31.
24. Pollock JL, Virgin HWt. Latency, without persistence, of murine cytomegalovirus in the spleen and kidney. J Virol. 1995;69(3):1762-8.
25. Tegtmeyer PK, Spanier J, Borst K, Becker J, Riedl A, Hirche C, et al. STING induces early IFN-β in the liver and constrains myeloid cell-mediated dissemination of murine cytomegalovirus. Nat Commun. 2019;10(1):2830.
26. Sacher T, Podlech J, Mohr CA, Jordan S, Ruzsics Z, Reddehase MJ, et al. The major virus-producing cell type during murine cytomegalovirus infection, the hepatocyte, is not the source of virus dissemination in the host. Cell host & microbe. 2008;3(4):263-72.
27. Kurz SK, Rapp M, Steffens HP, Grzimek NK, Schmalz S, Reddehase MJ. Focal transcriptional activity of murine cytomegalovirus during latency in the lungs. J Virol. 1999;73(1):482-94.
28. Kurz S, Steffens HP, Mayer A, Harris JR, Reddehase MJ. Latency versus persistence or intermittent recurrences: evidence for a latent state of murine cytomegalovirus in the lungs. J Virol. 1997;71(4):2980-7.
29. Chaudhry MZ, Casalegno-Garduno R, Sitnik KM, Kasmapour B, Pulm AK, Brizic I, et al. Cytomegalovirus inhibition of extrinsic apoptosis determines fitness and resistance to cytotoxic CD8 T cells. Proc Natl Acad Sci U S A. 2020;117(23):12961-8.
30. Munks MW, Rott K, Nesterenko PA, Smart SM, Williams V, Tatum A, et al. CD8 T Cell Memory Inflation is Driven by Latent CMV Infection of Lymphatic Endothelial Cells. bioRxiv. 2022:2022.02.10.479848.
31. Loewendorf AI, Arens R, Purton JF, Surh CD, Benedict CA. Dissecting the requirements for maintenance of the CMV-specific memory T-cell pool. Viral Immunol. 2011;24(4):351-5.
32. Stevens JG, Haarr L, Porter DD, Cook ML, Wagner EK. Prominence of the herpes simplex virus latency-associated transcript in trigeminal ganglia from seropositive humans. J Infect Dis. 1988;158(1):117-23.
33. Umbach JL, Kramer MF, Jurak I, Karnowski HW, Coen DM, Cullen BR. MicroRNAs expressed by herpes simplex virus 1 during latent infection regulate viral mRNAs. Nature. 2008;454(7205):780-3.

34. Rainbow L, Platt GM, Simpson GR, Sarid R, Gao SJ, Stoiber H, et al. The 222- to 234-kilodalton latent nuclear protein (LNA) of Kaposi's sarcoma-associated herpesvirus (human herpesvirus 8) is encoded by orf73 and is a component of the latency-associated nuclear antigen. J Virol. 1997;71(8):5915-21.
35. Hennessy K, Kieff E. A second nuclear protein is encoded by Epstein-Barr virus in latent infection. Science (New York, NY). 1985;227(4691):1238-40.
36. Goodrum F, Reeves M, Sinclair J, High K, Shenk T. Human cytomegalovirus sequences expressed in latently infected individuals promote a latent infection in vitro. Blood. 2007;110(3):937-45.
37. Reeves MB, Coleman H, Chadderton J, Goddard M, Sissons JG, Sinclair JH. Vascular endothelial and smooth muscle cells are unlikely to be major sites of latency of human cytomegalovirus in vivo. The Journal of general virology. 2004;85(Pt 11):3337-41.
38. Chung MI, Bujnis M, Barkauskas CE, Kobayashi Y, Hogan BLM. Niche-mediated BMP/SMAD signaling regulates lung alveolar stem cell proliferation and differentiation. Development. 2018;145(9).
39. Jordan S, Krause J, Prager A, Mitrovic M, Jonjic S, Koszinowski UH, et al. Virus progeny of murine cytomegalovirus bacterial artificial chromosome pSM3fr show reduced growth in salivary Glands due to a fixed mutation of MCK-2. J Virol. 2011;85(19):10346-53.
40. Oduro JD, Redeker A, Lemmermann NAW, Ebermann L, Marandu TF, Dekhtiarenko I, et al. Murine cytomegalovirus (CMV) infection via the intranasal route offers a robust model of immunity upon mucosal CMV infection. J Gen Virol. 2016;97(1):185-95.
41. Brizić I, Šušak B, Arapović M, Huszthy PC, Hiršl L, Kveštak D, et al. Brain-resident memory CD8(+) T cells induced by congenital CMV infection prevent brain pathology and virus reactivation. Eur J Immunol. 2018;48(6):950-64.
42. Sitnik KM, Wendland K, Weishaupt H, Uronen-Hansson H, White AJ, Anderson G, et al. Context-Dependent Development of Lymphoid Stroma from Adult CD34(+) Adventitial Progenitors. Cell Rep. 2016;14(10):2375-88.
43. Mederacke I, Dapito DH, Affo S, Uchinami H, Schwabe RF. High-yield and high-purity isolation of hepatic stellate cells from normal and fibrotic mouse livers. Nat Protoc. 2015;10(2):305-15.
44. Cossarizza A, Chang HD, Radbruch A, Abrignani S, Addo R, Akdis M, et al. Guidelines for the use of flow cytometry and cell sorting in immunological studies (third edition). Eur J Immunol. 2021;51(12):2708-3145.
45. Messerle M, Crnkovic I, Hammerschmidt W, Ziegler H, Koszinowski UH. Cloning and mutagenesis of a herpesvirus genome as an infectious bacterial artificial chromosome. Proceedings of the National Academy of Sciences of the United States of America. 1997;94(26):14759-63.
46. Tischer BK, Smith GA, Osterrieder N. En passant mutagenesis: a two step markerless red recombination system. Methods Mol Biol. 2010;634:421-30.
47. Rand U, Kubsch T, Kasmapour B, Cicin-Sain L. A Novel Triple-Fluorescent HCMV Strain Reveals Gene Expression Dynamics and Anti-Herpesviral Drug Mechanisms. Front Cell Infect Microbiol. 2021;10:536150.